

# INTER-SLICE SUPER-RESOLUTION OF MAGNETIC RESONANCE IMAGES BY PRE-TRAINING AND SELF-SUPERVISED FINE-TUNING

Xin Wang<sup>1,†</sup>    Zhiyun Song<sup>1,†</sup>    Yitao Zhu<sup>2</sup>    Sheng Wang<sup>1,4</sup>  
 Lichi Zhang<sup>1</sup>    Dinggang Shen<sup>2,3,4</sup>    Qian Wang<sup>2,3</sup>

<sup>1</sup> School of Biomedical Engineering, Shanghai Jiao Tong University, Shanghai, 200030, China

<sup>2</sup> School of Biomedical Engineering & State Key Laboratory of Advanced Medical Materials and Devices, ShanghaiTech University, Shanghai, 201210, China

<sup>3</sup> Shanghai Clinical Research and Trial Center, Shanghai, 201210, China

<sup>4</sup> Shanghai United Imaging Intelligence Co., Ltd., Shanghai, 200230, China

In clinical practice, 2D magnetic resonance (MR) sequences are widely adopted. While individual 2D slices can be stacked to form a 3D volume, the relatively large slice spacing can pose challenges for both image visualization and subsequent analysis tasks, which often require isotropic voxel spacing. To reduce slice spacing, deep-learning-based super-resolution techniques are widely investigated. However, most current solutions require a substantial number of paired high-resolution and low-resolution images for supervised training, which are typically unavailable in real-world scenarios. In this work, we propose a self-supervised super-resolution framework for inter-slice super-resolution of MR images. Our framework is first featured by pre-training on video dataset, as temporal correlation of videos is found beneficial for modeling the spatial relation among MR slices. Then, we use public high-quality MR dataset to fine-tune our pre-trained model, for enhancing awareness of our model to medical data. Finally, given a target dataset at hand, we utilize self-supervised fine-tuning to further ensure our model works well with user-specific super-resolution tasks. The proposed method demonstrates superior performance compared to other self-supervised methods and also holds the potential to benefit various downstream applications.

**Index Terms**— Super-resolution, Magnetic Resonance Image, Pre-training

## 1. INTRODUCTION

Magnetic resonance (MR) imaging is widely used for its non-invasive and detailed visualization of the human body. In clinical MR imaging, 2D sequences are widely employed for faster image acquisition, where multiple 2D slices can be stacked to create a 3D volume. Such volume typically has large inter-slice spacing, in contrast to the fine-grained intra-slice spacing [1]. The anisotropic voxel spacing in 3D can

pose significant challenges for many automatic image processing software requiring isotropic voxel spacing as input.

One straightforward solution is to resample the volume. However, this operation can corrupt images by blurring or aliasing, particularly near the boundaries of organ/tissue with sharp intensity transitions. Recently, several super-resolution (SR) techniques based on deep learning have been proposed [2–7]. A common idea of these methods is to leverage the power of neural networks to learn a mapping from the low-resolution (*LR*, with large inter-slice spacing) images to the high-resolution (*HR*, with small inter-slice spacing) ones.

To establish the mapping, supervised learning is a straightforward paradigm [2–4]. During training, the model takes an LR image as input and minimizes the discrepancy between the predicted and real HR image. However, the above paradigm faces the challenge that HR images sometimes cannot be acquired in clinical practice. To avoid using real HR data for supervision, researchers have developed self-supervised solutions, which can be divided into two categories: resampling-based and synthesis-based methods. The resampling-based methods [5, 6] first simulate images of lower resolution from original LR ones, learn a mapping from the lower-resolution images to the LR images, and then apply it to the LR images to predict the HR images. The synthesis-based methods [7] involve synthesizing HR images from the original LR images and training the SR model based on the synthesized images.

The main drawbacks of current self-supervised SR methods lie in limited training data and indirect mapping. Specifically, the training set is derived from a few LR cases. And the SR mapping is learned from lower-resolution to low-resolution data, or from synthesized LR to synthesized HR data, rather than the real LR-HR pairs, which could significantly impede the model’s performance. One potential solution is to pre-train on extensive public datasets [8], which offer strong initialization with high-quality data and alleviate the requirements for downstream data. Considering that medical images are comparably difficult to collect, several

† Equal contribution to this work.

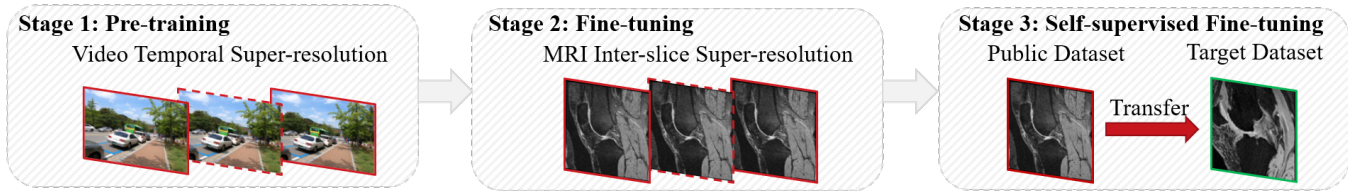


**Fig. 1.** The proposed three-stage super-resolution framework, combining advantages of pre-training, fine-tuning, and self-supervised fine-tuning.

studies [9, 10] explored the use of video datasets as an alternative to medical images for capturing inter-slice correlation.

This paper presents a novel SR framework that combines the advantages of supervised pre-training on public data and self-supervised fine-tuning on user-specific data. The pre-training offers high performance and generalization, and the fine-tuning further enables the model to adapt to specific data and task. As depicted in Fig. 1, the proposed framework consists of three stages: (1) *Pre-training on video frame interpolation*. It shares similarity with inter-slice SR of MR images as both tasks involve predicting intermediate frames/slices. Pre-training on abundant video data equips the model with strong prior for modeling the inter-slice correlation. (2) *Fine-tuning on high-quality MR dataset*. The motivation is to adapt the pre-trained model to the domain of medical images. Thus, it becomes familiar with MR-specific context, enhancing its performance in MR image representation. (3) *Self-supervised fine-tuning on target dataset*. Since the user-provided target dataset may have varying tissue types, modalities, or structural complexity, it is essential to adapt the model to user-specific cases through self-supervised fine-tuning.

The main contributions in this paper are listed as follows.

- We propose a framework for MR inter-slice SR that benefits from pre-training on abundant video data.
- We adapt the pre-trained SR model to user cases by self-supervised fine-tuning.
- We demonstrate superior SR performance over other self-supervised methods on knee MR images.

## 2. METHODOLOGY

Our method contains three parts: (1) pre-training on video frame interpolation, (2) fine-tuning on high-quality MR dataset for transferring the pre-trained model to MR images, and (3) self-supervised fine-tuning on target dataset for further transferring to user cases.

### 2.1. Pre-training on Video Frame Interpolation

Video pre-training is found to be beneficial for 3D medical tasks [11]. Although numerous pre-trained video models are publicly available, most are specialized for discriminative tasks, such as video classification and action recognition. Consequently, they may not effectively capture fine-grained

features required by generative tasks. In our case, we find that directly deploying a public pre-trained video classification model yields no improvement in the performance of downstream SR task. Therefore, we first pre-train the SR model on video frame interpolation task.

We adopt SA-INR [4] as the SR model, which parameterizes a frame or slice sequence as a continuous function of spatial coordinates. The training process is illustrated as follows. First, we randomly choose a sub-sequence  $I_{seq}$  with a length of  $15n + 1$ , retaining one frame for every  $n$  and taking the rest as ground truth. Here  $n$  denotes the down-sampling factor. Given two adjacent frames  $I^i, I^{i+n} \in I_{seq}$ , we synthesize an intermediate frame  $I^{i+k}$  ( $0 \leq k \leq n$ ). To achieve this goal, we input  $I^i$  and  $I^{i+n}$ , as well as the spatial coordinates  $C^{i+k}$  of frame  $I^{i+k}$ , to SA-INR, which will return a predicted intermediate frame  $\hat{I}^{i+k}$ . Finally, we calculate the  $L_1$  loss to enforce the pixel-wise consistency between the predicted frame  $\hat{I}^{i+k}$  and the real intermediate frame  $I^{i+k}$ :

$$\begin{aligned} L &= \|\hat{I}^{i+k} - I^{i+k}\| \\ &= \|\mathcal{F}(I^i, I^{i+n}, C^{i+k}) - I^{i+k}\|, \end{aligned}$$

where  $\mathcal{F}(\cdot)$  denotes the mapping function of the SR network.

By reconstructing the missing temporal frames, the model not only effectively captures fine-grained visual cues, but also learns spatio-temporal information in the video that mimics inter-slice relation in an MR volume.

### 2.2. Fine-tuning on High-quality MR Dataset

In the second stage, we transfer the SR model pre-trained on the video dataset to the MR domain. This fine-tuning enables the model to capture the essential anatomical characteristics by learning from high-quality MR images. Note that the high-quality MR images here are relatively costly to acquire, thus NOT widely used in clinical practice. We utilize these images to supervise the fine-tuning of the SR model.

After pre-training the SR model on the video frame interpolation task, we fine-tune all the parameters of the model on the MR inter-slice SR task. Specifically, for each iteration of training, we randomly select an HR volume  $I_{HR}$  with spatial resolution of  $a \times a \times a$  from the training set. Then we down-sample the volume along the  $z$ -axis and obtain an LR volume  $I_{LR}$  with spatial resolution of  $a \times a \times na$  where  $n$  represents

**Table 1.** Quantitative results for different self-supervised super-resolution methods on the SKI10 dataset.

Method	PSNR		SSIM	
	Mean	SD	Mean	SD
Trilinear	28.26	2.59	0.8108	0.0468
TSCNet [6]	27.37	2.46	0.7841	0.0478
SMORE [5]	29.33	2.76	0.8450	0.0434
Xuan <i>et al.</i> [7]	30.39	2.82	0.8425	0.0471
Proposed	<b>30.88</b>	2.83	<b>0.8517</b>	0.0512
Supervised	31.22	2.83	0.8628	0.0471

the downsampling factor. Next, we extract two adjacent slices  $S_{x,y}^i$  and  $S_{x,y}^{i+n}$  from  $I_{HR}$  as the input of SA-INR, and reconstruct the desired middle slice  $\hat{S}_{x,y}^{i+k}$  ( $0 \leq k \leq n$ ). Finally, we calculate and minimize the loss between  $\hat{S}_{x,y}^{i+k}$  and the real intermediate slice  $S_{x,y}^{i+k}$ .

### 2.3. Self-supervised Fine-tuning on Target Dataset

Finally, we conduct self-supervised fine-tuning on the target dataset. This step is essential because directly applying the SR model trained on public dataset to specific user cases may lead to performance decrease due to domain gap. Regarding fine-tuning, the difference between Stage 2 and Stage 3 is that only LR images are available to fine-tune Stage 3, while real HR images are available to supervise Stage 2. Thus, to acquire HR-LR pairs for Stage 3, we further downsample the LR images in the target dataset. Specifically, to enable tailored solution for each single subject, we conduct subject-based fine-tuning here. Given an LR volume  $I_{LR}$  with spatial resolution of  $a \times a \times c$  ( $c \geq a$ ), we downsample the volume along  $x$ -axis (or  $y$ -axis) to acquire  $I_{LR,x\downarrow}$  with spatial resolution of  $na \times a \times c$ , where  $n$  represents the downsampling factor. In this way, we can build a training set  $\{I_{LR}, I_{LR,x\downarrow}\}$ .

We investigate several fine-tuning strategies, including fine-tuning all parameters, freezing a subset of parameters, and employing the parameter-efficient fine-tuning technique (PEFT) [12]. Our experiments reveal that fine-tuning all parameters (2.1M) is the most effective and does not impose significant computational resource burden. The subject-based fine-tuning takes about 1 minute on an A100 40G card, and the subsequent SR process takes about 20 seconds.

## 3. EXPERIMENTS

### 3.1. Datasets and Experimental Setup

**Video Dataset:** We use the REDS-VTSR dataset [13] for pre-training, which consists of 270 sequences with a frame rate of 60fps. Each sequence contains 180 frames with a size of  $720\text{px} \times 1280\text{px}$ . We have found that long sequences are more conducive to our task since they contain richer temporal information. During training, we transform each RGB frame

**Table 2.** Quantitative results for the ablation study. VP denotes pre-training on video, SF denotes supervised fine-tuning on MRI dataset, and SSF denotes self-supervised fine-tuning on target dataset.

VP	SF	SSF	PSNR		SSIM	
			Mean	SD	Mean	SD
	✓		30.19	2.77	0.8216	0.0591
	✓	✓	30.40	2.78	0.8342	0.0569
✓	✓		30.73	2.80	0.8404	0.0540
✓	✓	✓	<b>30.88</b>	2.83	<b>0.8517</b>	0.0512

to gray, resize it to  $90\text{px} \times 160\text{px}$  and then crop a  $64\text{px} \times 64\text{px}$  patch. We pre-train our model on the REDS-VTSR dataset for 1000 epochs with an initial learning rate of  $1e^{-4}$ , which is halved every 200 epochs.

**Public MR Dataset:** We adapt the pre-trained video SR model to the publicly available Osteoarthritis Initiative (OAI) dataset [14]. Specifically, we collect a total of 350 cases (3D DESS, spatial resolution:  $0.3646\text{mm} \times 0.3646\text{mm} \times 0.7\text{mm}$ ), where 300 cases are used for training and 50 cases for validation. During training, we randomly crop an HR patch with a size of  $64 \times 64 \times 16n$  for each case, from which we simulate an LR patch ( $64 \times 64 \times 16$ ) following [15]. We fine-tune the model on the OAI dataset for 1000 epochs, using the same experimental settings as in the pre-training phase.

**Target MR Dataset:** We perform self-supervised fine-tuning on the Segmentation of Knee Images 2010 (SKI10) dataset [16]. We collect 150 cases (100 for training, 50 for testing) with T1 or T2-weighted modalities. All images are scanned in the sagittal plane with the spatial resolution of  $0.4\text{mm} \times 0.4\text{mm} \times 1.0\text{mm}$ . We downsample them by 4 times to simulate LR data with resolution of  $0.4\text{mm} \times 0.4\text{mm} \times 4.0\text{mm}$ . Note that the supervised method is trained using the training set of SKI10 and evaluated on the testing set. In contrast, the self-supervised methods are trained and evaluated solely on the testing set, without referencing to any HR images. For each case, we randomly extract 100 patches and fine-tune the SR model for 5 epochs.

**Comparison Methods:** We compare our method with three self-supervised SR methods: (1) TSCNet [6], a two-stage method that first initiates the network by through-plane LR-HR pairs, and then refines the network using cyclic-based interpolation; (2) SMORE [5], which first degrades sagittal slices and trains a 2D neural network on sagittal pairs, and then applies it to reconstruct HR coronal and axial views; (3) Xuan *et al.* [7], which synthesizes HR image using the variational auto-encoder [17], and trains a super-resolution network based on these synthesized pairs.

### 3.2. Comparative Results on SKI10

We conduct quantitative evaluation using two commonly used metrics, *i.e.*, the Peak Signal-to-Noise Ratio (PSNR)

and Structural Similarity (SSIM) [18], and also provide the qualitative results. As reported in Table 1, almost all of the self-supervised methods outperform the baseline of trilinear resampling, except for TSCNet. We also observe the impressive PSNR produced by Xuan *et al.* However, the SSIM results produced by Xuan *et al.* are inferior, as there are some distorted structures, as confirmed by red boxes in Fig. 2. Instead, our method reconstructs the most reliable MR images. By leveraging the combined benefits of supervised pre-training and self-supervised fine-tuning, the resulting images exhibit superior quality, showcasing enhanced inter-slice continuity and fidelity. We also perform the supervised SR on the training set of SKI10 and report the metrics on the test set. It is inspiring to find that our method is close to this upper bound, with a margin of only 0.34dB in terms of PSNR.

### 3.3. Ablation Study

We evaluate the impact of Video Pre-training (VP) and Self-supervised Fine-tuning (SSF) by combining each of them with Supervised Fine-tuning (SF) on the same dataset. As reported in Table 2, some important findings are observed.

#### 3.3.1. Video Pre-training Benefits MRI Super-Resolution

To evaluate the benefits brought by video pre-training, we start with supervised training on OAI. As denoted by the VP+SF row in Table 2, there is a significant performance improvement when using video pre-training to initialize the SR model. This indicates that video pre-training can benefit downstream MR inter-slice SR task, probably due to the following two reasons. First, video frames are sequential data in nature and exhibit temporal consistency; pre-training on video frame interpolation task helps the SR model capture and leverage this temporal information, which is particularly beneficial when dealing with MR volume, where inter-slice connection is crucial. Second, by pre-training from abundant video data, an SR model can learn to extract a wealth of visual information, which not only enhances the quality of MR images, but also accelerates the convergence of the SR model during fine-tuning on MR data, reducing the need for extensive training on the medical data.

#### 3.3.2. Self-supervised Fine-tuning Ensures the Adaptation to Specific Cases

Given the intricate structural and modal nuances of MR images, the models trained on specific public datasets may face challenges when generalizing to complex cases during evaluation. As shown in Table 2, the performance of supervised training on the OAI dataset is even inferior to most of the self-supervised training methods on the target SKI10 dataset, particularly in terms of SSIM. After performing the subject-based self-supervised fine-tuning, the SR model successfully adapts to the target dataset and yields significantly superior

results. Moreover, the best results are achieved when combining the two strategies (VP and SSF) together, as denoted by the VP+SF+SSF row.

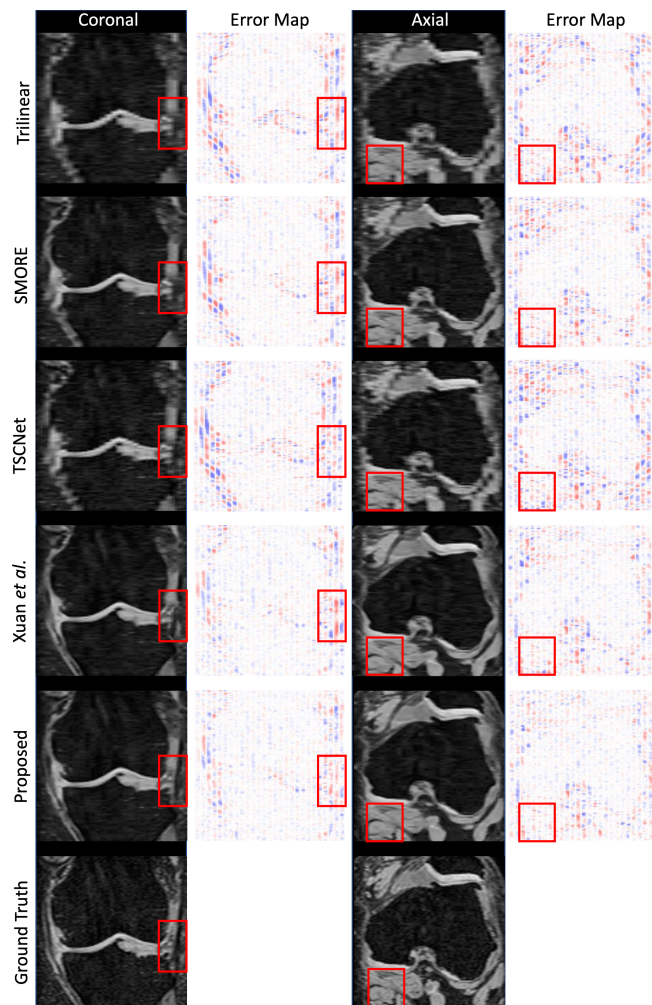


Fig. 2. Qualitative results and error maps for different self-supervised SR methods on the SKI10 dataset.

## 4. CONCLUSION

In summary, our three-stage self-supervised framework offers a compelling solution to the challenge of implementing SR in clinical settings where HR data is absent. By combining supervised pre-training on high-quality dataset and self-supervised fine-tuning on target dataset, we achieve superior results compared to state-of-the-art methods.

Meanwhile, we demonstrate the effectiveness of video pre-training for MR modeling, bridging the task gap between video temporal SR and MR inter-slice SR. Given the scarcity of medical data in contrast to the abundance of video data, there is a promising potential for improving 3D medical task through video pre-training.

## 5. COMPLIANCE WITH ETHICAL STANDARDS

This research study was conducted retrospectively using human subject data made available in open access. Ethical approval was not required as confirmed by the license attached with the open access data.

## 6. REFERENCES

- [1] Dominik Weishaupt, Victor D Köchli, Borut Marincek, Johannes M Froehlich, Daniel Nanz, and Klaas P Pruessmann, *How does MRI work?: an introduction to the physics and function of magnetic resonance imaging*, vol. 2, Springer, 2006.
- [2] Qing Wu, Yuwei Li, Yawen Sun, Yan Zhou, Hongjiang Wei, Jingyi Yu, and Yuyao Zhang, “An arbitrary scale super-resolution approach for 3d mr images via implicit neural representation,” *IEEE Journal of Biomedical and Health Informatics*, vol. 27, no. 2, pp. 1004–1015, 2023.
- [3] Akshay S Chaudhari, Zhongnan Fang, Feliks Kogan, Jeff Wood, Kathryn J Stevens, Eric K Gibbons, Jin Hyung Lee, Garry E Gold, and Brian A Hargreaves, “Super-resolution musculoskeletal mri using deep learning,” *Magnetic Resonance in Medicine*, vol. 80, no. 5, pp. 2139–2154, 2018.
- [4] Xin Wang, Kai Xuan, Sheng Wang, Honglin Xiong, Lichi Zhang, and Qian Wang, “Arbitrary reduction of mri slice spacing based on local-aware implicit representation,” *arXiv preprint arXiv:2205.11346*, 2022.
- [5] Can Zhao, Blake E. Dewey, Dzung L. Pham, Peter A. Calabresi, Daniel S. Reich, and Jerry L. Prince, “Smore: A self-supervised anti-aliasing and super-resolution algorithm for mri using deep learning,” *IEEE Transactions on Medical Imaging*, vol. 40, no. 3, pp. 805–817, 2021.
- [6] Zhiyang Lu, Zheng Li, Jun Wang, Jun Shi, and Dinggang Shen, “Two-stage self-supervised cycle-consistency network for reconstruction of thin-slice mr images,” in *International Conference on Medical Image Computing and Computer Assisted Intervention*. 2021, pp. 3–12, Springer.
- [7] Kai Xuan, Liping Si, Lichi Zhang, Zhong Xue, Yining Jiao, Weiwu Yao, Dinggang Shen, Dijia Wu, and Qian Wang, “Reducing magnetic resonance image spacing by learning without ground-truth,” *Pattern Recognition*, vol. 120, pp. 108103, 2021.
- [8] Sihong Chen, Kai Ma, and Yefeng Zheng, “Med3d: Transfer learning for 3d medical image analysis,” *arXiv preprint arXiv:1904.00625*, 2019.
- [9] Pranav Rajpurkar, Allison Park, Jeremy Irvin, Chris Chute, Michael Bereket, Domenico Mastrodicasa, Curtis P Langlotz, Matthew P Lungren, Andrew Y Ng, and Bhavik N Patel, “Appendixnet: deep learning for diagnosis of appendicitis from a small dataset of ct exams using video pretraining,” *Scientific Reports*, vol. 10, no. 1, pp. 3958, 2020.
- [10] Alexander Ke, Shih-Cheng Huang, Chloe P O’Connell, Michal Klimont, Serena Yeung, and Pranav Rajpurkar, “Video pretraining advances 3d deep learning on chest ct tasks,” *arXiv preprint arXiv:2304.00546*, 2023.
- [11] Alexander Ke, Shih-Cheng Huang, Chloe P O’Connell, Michal Klimont, Serena Yeung, and Pranav Rajpurkar, “Video pretraining advances 3d deep learning on chest CT tasks,” in *Medical Imaging with Deep Learning*, 2023.
- [12] Edward J Hu, Yelong Shen, Phillip Wallis, Zeyuan Allen-Zhu, Yuanzhi Li, Shean Wang, Lu Wang, and Weizhu Chen, “Lora: Low-rank adaptation of large language models,” *arXiv preprint arXiv:2106.09685*, 2021.
- [13] Seungjun Nah et al., “Aim 2019 challenge on video temporal super-resolution: Methods and results,” in *2019 IEEE/CVF International Conference on Computer Vision Workshop (ICCVW)*, 2019, pp. 3388–3398.
- [14] “Oai dataset,” <https://nda.nih.gov/oai/>. Accessed: 2022-11-21.
- [15] Juan Eugenio Iglesias, Benjamin Billot, Yaël Balbastre, Azadeh Tabari, John Conklin, R Gilberto González, Daniel C Alexander, Polina Golland, Brian L Edlow, Bruce Fischl, et al., “Joint super-resolution and synthesis of 1 mm isotropic mp-rage volumes from clinical mri exams with scans of different orientation, resolution and contrast,” *Neuroimage*, vol. 237, pp. 118206, 2021.
- [16] Tobias Heimann, Bryan J Morrison, Martin A Styner, Marc Niethammer, and Simon Warfield, “Segmentation of knee images: a grand challenge,” in *Proc. MICCAI Workshop on Medical Image Analysis for the Clinic*. Beijing, China, 2010, vol. 1.
- [17] Diederik P Kingma and Max Welling, “Auto-encoding variational bayes,” *arXiv preprint arXiv:1312.6114*, 2013.
- [18] Z. Wang, E.P. Simoncelli, and A.C. Bovik, “Multi-scale structural similarity for image quality assessment,” in *The Thirty-Seventh Asilomar Conference on Signals, Systems & Computers, 2003*, 2003, vol. 2, pp. 1398–1402 Vol.2.